Bulgarian Chemical Communications, Volume 50, Special Issue F (pp. 143–149) 2018

The influence of the modification of zirconium tungstate with Eu(III) on the α → β phase transition temperature and optical band gap

E. D. Encheva, M. K. Nedyalkov, M. P. Tsvetkov, M. M. Milanova*

University of Sofia "St. Kl. Ohridski", Faculty of Chemistry and Pharmacy, Department of Inorganic Chemistry, Laboratory of rare and rare earth elements, 1 J. Bourchier Blvd., 1164 Sofia, Bulgaria

Received October 22, 2018; Accepted December 01, 2018

The hydrothermal method was used to obtain pure and Eu(III)-modified ZrW_2O_8. Tungstates modified with 1, 2, and 5 mol% Eu(III) were synthesized in order to investigate the influence of Eu(III) doping on the properties of zirconium tungstate. The samples obtained were phase homogeneous as shown by XRD. High temperature XRD was used to follow the temperature of the alpha-beta phase transition. It was observed that the higher the content of Eu(III), the higher the temperature of the transition. The unit cell parameters decrease both with the Eu(III) content and the temperature increasing. The values of the thermal expansion coefficients obtained decreased with increasing Eu(III) for both the alpha and beta phases of ZrW_2O_8. Doping with increasing amounts of Eu(III) increased the energy of the optical band gap as well.

Keywords: zirconium tungstate, Eu(III) modification, XRD, phase transition, band gap energy.

INTRODUCTION

In the recent years the modification of tungstates isostructural with $CaWO_4$ was studied for their potential application for light emitting diodes [1–3]. Among those studied is the tungstate $NaY(WO_4)_2$, where Y^{3+} can be substituted by other lanthanide ions, Ln^{3+}, due to their similar ionic radii [3]; $NaLn(WO_4)_2$ can be additionally co-doped with other Ln^{3+} [4]. However, because the materials mentioned have a positive coefficient of thermal expansion (CTE) and the impurities (sources of luminescence) worsen the mechanical properties, they cannot operate in an environment with large temperature changes. Therefore, potential replacements could be the tungstates of Zr and Hf, which have negative coefficients of thermal expansion [5–8].

The cubic ZrW_2O_8 (primitive cubic space group $P2_13$, $a = 9.1600$ Å, PDF 00-050-1868) is the subject of interest in the research presented here. Its negative thermal expansion (-10.2×10^{-6} K^{-1}, 30–120 °C [9]) is isotropic and relatively constant over a wide temperature range of –273 °C to 777 °C. In this range, the phase transition α-ZrW_2O_8 → β-ZrW_2O_8 occurs (primitive cubic space group $Pa\bar{3}$, $a = 9.1371$ [5]) that is associated with an order-disorder transition. The temperature of the transition is not well defined and in the literature the values for it vary in the range between 157 °C and 175 °C [10]. Heating above 777 °C can lead to the decomposition of the compound to its constituent oxides, ZrO_2 and WO_3 [6, 7].

Although the crystal lattice is flexible with respect to temperature changes, the literature data show that the cations in ZrW_2O_8 are difficult to substitute in both cationic sublattices [8]. The only complete substitution in the zirconium sublattice is with Hf in $Zr_{1-x}Hf_xW_2O_8$ [5, 11]. The ions Ti^{4+} and Sn^{4+} were studied as possible substituting ions for the Zr^{4+} position in ZrW_2O_8. Attempts to replace Zr have resulted in the substitution of only 30% for Sn^{4+} [12] and 5% for Ti^{4+} cations [13]. Substitution studies indicate that isomorphic solid solutions are obtained, described by the general formula $ZrW_{1-x}Ti_xO_8$ [13, 14]. There are no reports in the literature of attempts to replace Zr with other tetravalent ions. Substitutions with lanthanide ions are limited to 5% and are only obtained for ions with small ionic radius. The literature data related to the preparation of ZrW_2O_8-based red phosphorus by modification with Eu^{3+} are limited [15].

Data on the influence of different modifiers on the properties of cubic tungstates are rather incomplete. It was found that even small amounts of a modifying agent may influence the phase transition temperature and the coefficient of thermal expan-

* To whom all correspondence should be sent:
E-mail: mariamilanova2@abv.bg, nhmm@wmail.chem.uni-sofia.bg

sion (CTE) [16]. The introduction of ions with different radius and charge can lead to a disorder in the crystalline structure of the tungstate and consequently to a change in their properties [8].

Although tungstates of Zr (as well as that of Hf) are difficult to produce, different methods have been successfully applied, among them coprecipitation [17], solid state reaction [18–22], low-temperature spark plasma sintering [23], sol gel method [9, 24], and hydrothermal synthesis [25–27]. Hydrothermal synthesis is considered suitable and economically advantageous because it is carried out at relatively low temperatures and produces phase homogeneous materials [27].

In the work presented here, the hydrothermal method was applied for zirconium tungstate synthesis and its modification with different contents of Eu(III). The influence of the temperature and the content of the modifying agent on the coefficient of thermal expansion were followed. The band gap energy was calculated in order to evaluate the potential application of the semiconductors obtained in photochemical processes.

EXPERIMENTAL

Materials

ACS grade starting materials $ZrOCl_2 \cdot 8H_2O$ (Sigma-Aldrich) and $Na_2WO_4 \cdot 2H_2O$ (Aldrich) were used. $Eu(NO_3)_3 \cdot nH_2O$ was synthesized from Eu_2O_3 (Fluka, p.a.) by dissolving it in heated dilute HNO_3, followed by crystallization after cooling of the solution. The amount of water of crystallization was determined by titration.

Synthetic procedure

Synthesis of pure ZrW_2O_8

Initial solutions of $ZrOCl_2 \cdot 8H_2O$ and $Na_2WO_4 \cdot 2H_2O$ in water with a concentration of 0.1 and 0.2 M, respectively, were prepared. They were mixed in stoichiometric ratio calculated Zr/W = 1:2, heated to 60 °C and stirred for 30 min. To the homogeneous solution obtained 15 ml 6M HCl was added (final concentration of HCl about 3M), followed by additional heating at 60 °C for 2 hours. After adding 5 ml of 1-butanol, the solution was heated in a 75 ml Teflon autoclave for 15 h at 180 °C while stirring. After cooling down to room temperature, the suspension obtained was filtered, washed with water and EtOH and dried at 50 °C. After calcination in preheated oven at 600 °C for 1 h and quick cooling down to room temperature, the sample obtained was ready for analysis.

Synthesis of ZrW_2O_8 modified with Eu(III)

A procedure analogous to the above for the pure ZrW_2O_8 was followed except that in the first step, a 0.01 M water solution of $Eu(NO_3)_3 \cdot nH_2O$ was added in such amount to obtain ZrW_2O_8 samples with 1, 2 and 5 mol% Eu(III).

Methods for characterization

High temperature XRD was performed using a PANalytical Empyrean diffractometer with PIXcel 3D detector. The XRD patterns were recorded between 15–90° 2θ with step 0.026°. An Anton Paar HTK 16N camera was used for *in situ* high temperature measurements in the interval 25–250 °C with different steps. The unit cell parameters were calculated by the least square method using the FullProf software [28]. For the starting model of the α-ZrW_2O_8 the structure provided by [29] was used, while for the β-phase the structure of $ZrWMoO_8$ which adopts the $Pa\bar{3}$ space group at room temperature [30] was used.

UV-VIS absorption spectroscopy – an Evolution 300 UV-Vis spectrometer (Thermo Scientific) was used for measuring the absorption of the samples in the range 200–900 nm.

Band gap energy calculations. The optical properties (absorption and optical band gap energy) of the samples were studied using UV-Vis absorption spectra. In all cases absorption was registered from 200 to 400 nm. The UV-Vis data were analyzed for the relation between the optical band gap, absorption coefficient and energy (hν) of the incident photon for near edge optical absorption in semiconductors. The band gap energy was calculated from the measured curves by fits according to Tauc's equation [31] $\alpha h\nu = A(h\nu - E_g)^{n/2}$, where A is a constant independent of $h\nu$, E_g is the semiconductor band gap and n depends on the type of transition. The value used for n was 1, reflecting a direct transition. The well-known approach for semiconductor band gap energy determination from the intersection of linear fits of $(\alpha h\nu)^{1/n}$ versus hν on the x-axis was used, where n can be 1/2 and 2 for direct and indirect band gap, respectively.

RESULTS AND DISCUSSION

Characterization of the samples by XRD phase analysis

The XRD patterns from the high temperature analysis from 25 to 250 °C for pure ZrW_2O_8 are presented in Figure 1. The Eu(III)-modified ZrW_2O_8 samples show the same tendency that is why their

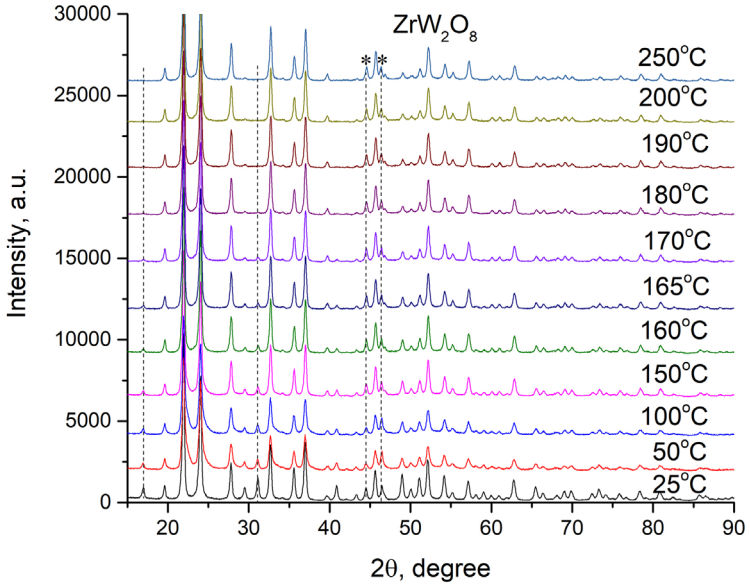

Fig. 1. XRD for pure ZrW_2O_8 at increasing temperature in the interval 25–250 °C; dashed lines illustrate the changes in the reflection peaks with the temperature. The asterisks denote Pt (111) and (002) reflections.

XRD patterns are not included in the text. The powder X-ray diffraction patterns of the samples proved their crystalline nature and the peaks matched well with literature ZrW_2O_8 reflections. All the diffractograms show the reflection peaks typical for ZrW_2O_8. No additional phases containing W or Zr are observed. The reflection peaks at 39.28 and 45.67 2θ, typical for Pt (111) and (002), respectively, are due to the substrate used during the measurements.

In order to observe *the phase transition α-ZrW_2O_8 → β-ZrW_2O_8*, the change in the intensity of the reflection peaks (110) and (310) was followed. These peaks are typical for the low-temperature α-ZrW_2O_8 but not for the high-temperature β-ZrW_2O_8 phase. The dashed lines in Figure 1 point out that with the temperature increase the intensity of these reflection peaks decreases and they disappear above the temperature of phase transition.

Based on the evolution of reflection peak (310) during the high temperature investigations, it can be concluded that the modification of ZrW_2O_8 with Eu(III) causes an increase of the phase transition temperature (Fig. 2). The absence of the reflection peak (310) in the diffraction pattern of the non-

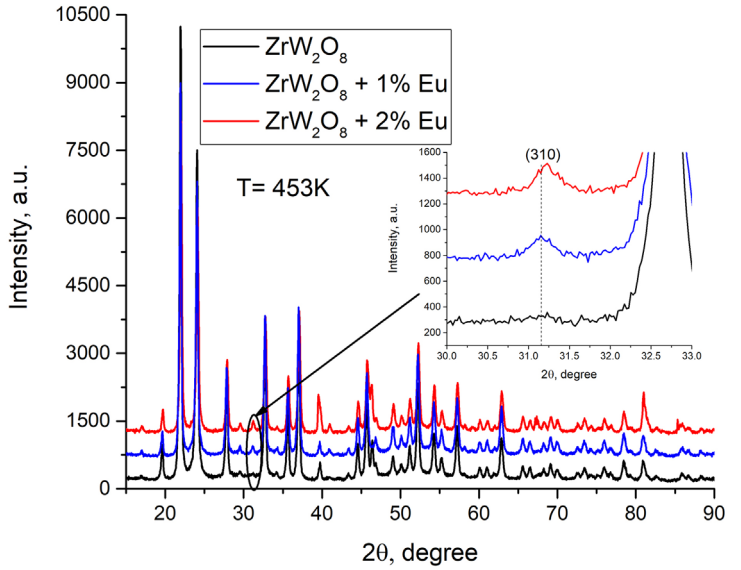

Fig. 2. Influence of Eu(III) on the increase of the phase transition temperature: XRD for ZrW_2O_8, pure and modified with 1 and 2 mol% Eu(III) at 453 K from bottom to top.

modified tungstate at 180°C (453 K) is evidence for the complete transition to β-ZrW_2O_8 phase. In the diffraction pattern of the ZrW_2O_8 modified with 1 and 2 mol% Eu(III) at that temperature the reflection peak (310) is still visible.

The phase transition along with the complete phase reverse α-$ZrW_2O_8 \rightleftharpoons \beta$-$ZrW_2O_8$ after cooling back to 25 °C is shown in Figure 3. The difference in the structure of α-ZrW_2O_8 and β-ZrW_2O_8 phases is also presented. For the low temperature α-ZrW_2O_8 phase the corner-sharing octahedra ZrO_6 and tetrahedra WO_4 are shown, each WO_4 tetrahedron shares three of its oxygen with the adjacent octahedra. In the high-temperature β-ZrW_2O_8 phase two crystallographic WO_4 share three joined O atoms [8].

It is known that *the transition* α-$ZrW_2O_8 \rightarrow \beta$-$ZrW_2O_8$, called order-to-disorder phase transition, depends on the orientation of WO_4 tetrahedra [5]. A *characteristic parameter* η'_T has been proposed to evaluate the extent of the disorder of WO_4 tetrahedra depending on the temperature [32]. The parameter can be calculated by the integrated intensity of the reflection peak (310) versus (210) with the formula

$$\eta'_T = \sqrt{\frac{[(I310/I210)]T}{[(I310/I210)\mathrm{ZrW2O8}]298K}} .$$

From Figure 4 it can be seen that in the presence of the modification agent Eu(III) the approach of the parameter η'_T value equal to zero i.e. complete disorder WO_4, is shifted to higher temperatures.

The dependence observed by us is different from the results published in the literature when the lanthanide ions are present in the structure of ZrW_2O_8 [32]. Quite likely the reason for the difference is the incomplete crystallization of our samples (small average crystallite size) as can be seen from the data in Table 1. The data show that the crystallites are growing during the measurements, which could cause an additional rearrangement of WO_4 and as a result a shift of the curve to higher temperatures is observed.

The *coefficients of thermal expansion* (CTE) calculated for the interval 25–100 °C (α-ZrW_2O_8 phase) and 200–250 °C (β-ZrW_2O_8 phase) are presented in Table 1. The calculations were made by the classical formula for linear thermal expansion:

$$\alpha = \frac{(a_{T2} - a_{T1})}{a_{T1}.\Delta T},$$

where α is the linear expansion coefficient, a_{T_1} and a_{T_2} are the unit cell parameters at low and high temperature, respectively and ΔT is the temperature difference.

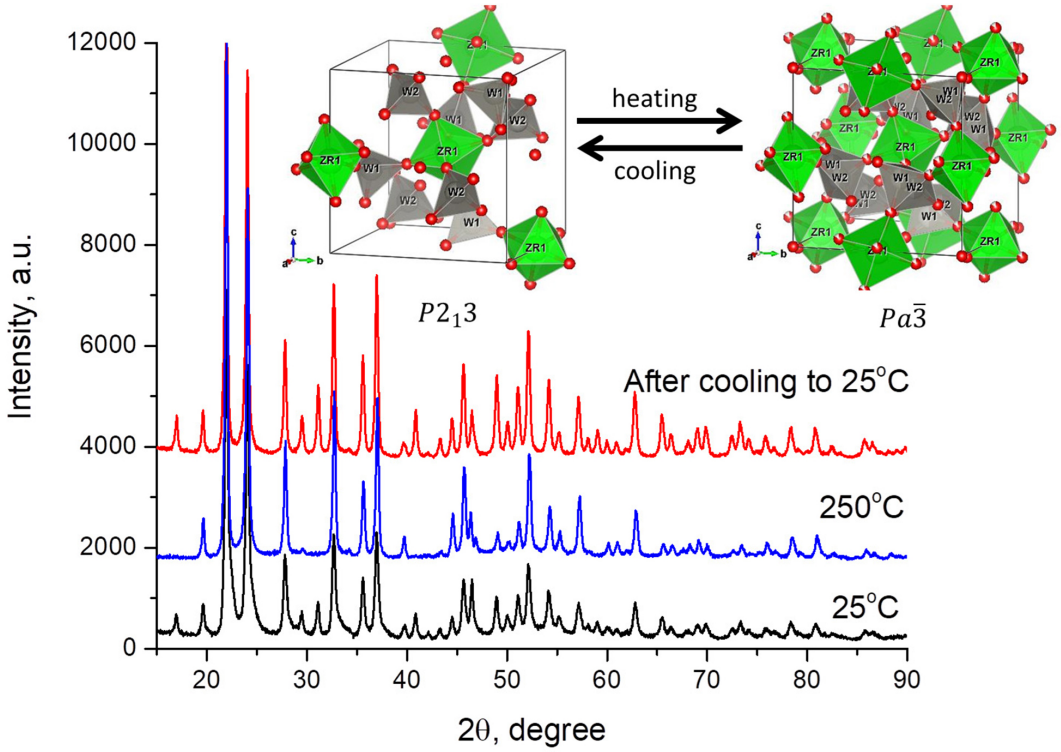

Fig. 3. Reversibility of the phase transition α-$ZrW_2O_8 \rightleftharpoons \beta$-$ZrW_2O_8$: XRD for ZrW_2O_8 at 25 and 250 °C, and after cooling at 25 °C, from bottom to top.

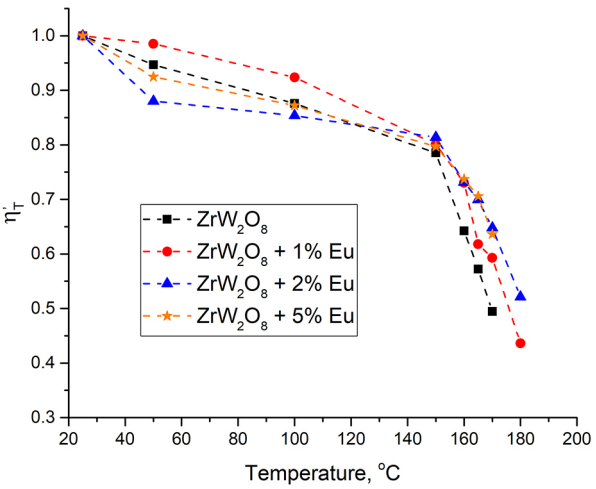

Fig. 4. Influence of the temperature and the modification agent Eu(III) on WO_4 tetrahedra disorder.

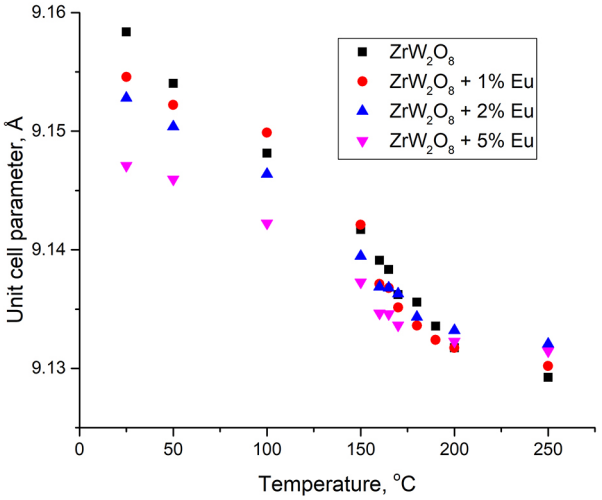

Fig.5. Unit cell parameter change with the Eu(III) content and the temperature.

It can be seen that the addition of Eu(III) caused a decrease in the CTE for both phases. The value for the α-ZrW_2O_8 phase is similar to literature data ($–10.2×10^{–6}$ $K^{–1}$, 30–120 °C [9]) even though a different synthesis procedure has been used.

The change of the *unit cell parameter* with the Eu(III) content and the temperature is presented in Figure 5. It can be seen that Eu(III) addition causes a decrease of the unit cell parameter. This can be explained by a partial replacement of Zr by Eu, leading to a solid solution of the type $Zr_{1–x}Eu_xW_2O_{8–x/2}$. The unit cell parameter decreases as a function of increasing temperature, which is to be expected due to the negative coefficient of thermal expansion (CTE) for ZrW_2O_8.

The band gap energy

The tungstates are semiconductors with a band gap energy for tungstates with formula AWO_4 in the interval 2.1–4.8 eV [33, 34]. The band gap energy for double tungstates of the type $AgLn(WO_4)_2$ show values between 3.48 to 4.00 eV for all Ln(III), including Y(III), for an indirect allowed transition [35].

The band gaps calculated on the base of the UV-Vis spectra are presented in Figure 6, assuming a transition of the direct type.

For the non-modified ZrW_2O_8 the value is 3.95 eV, while for the samples modified with 1 and 2 mol% Eu(III) the band gap is broader, with practically the same energy of 4.33 eV. For the sample with 5 mol% Eu(III) the energy band gap increased to 4.45 eV. The values are high and clearly increase with increasing Eu(III) content. So far the position of the Eu(III) in the structure of the tungstate is not determined. Considering that it changed the lattice parameters (Fig. 5), its present in the crystal structure could be suggested. It is quite likely to be present on the surface of the sample, as well. So far

Table 1. The crystallites size and the coefficients of temperature expansion, CTE

		ZrW_2O_8	ZrW_2O_8 + 1% Eu	ZrW_2O_8 + 2% Eu	ZrW_2O_8 + 5% Eu
Crystallites size	25 °C	26 nm	24 nm	20 nm	19 nm
	250 °C	31 nm	28 nm	29 nm	26 nm
	25 °C after cooling	31 nm	28 nm	29 nm	26 nm
CTE	25–100 °C	$–10.8×10^{–6}$ $K^{–1}$	$–7.4×10^{–6}$ $K^{–1}$	$–9.3×10^{–6}$ $K^{–1}$	$–8.5×10^{–6}$ $K^{–1}$
	200–250 °C	$–5.4×10^{–6}$ $K^{–1}$	$–3.6×10^{–6}$ $K^{–1}$	$–2.8×10^{–6}$ $K^{–1}$	$–2.5×10^{–6}$ $K^{–1}$
Unit cell parameter, Å	25 °C	9.15700(9)	9.15499(2)	9.15281(8)	9.14788(13)
	100 °C	9.14956(5)	9.14997(7)	9.14639(6)	9.14205(9)
	200 °C	9.13174(3)	9.13172(11)	9.13322(4)	9.13209(15)
	250 °C	9.12925(10)	9.13009(7)	9.13192(12)	9.13094(6)

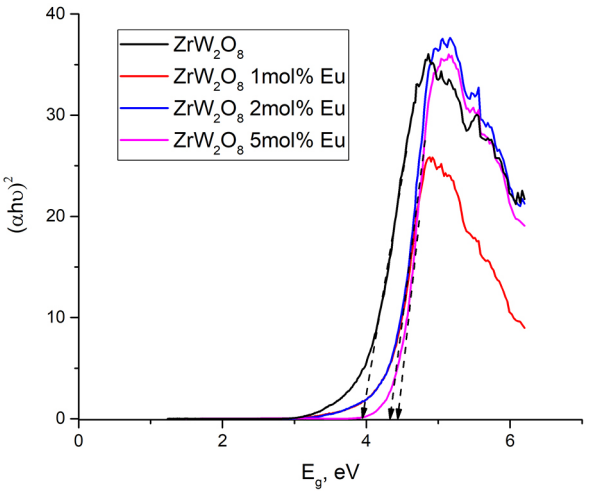

Fig. 6. The energy band gap.

it is difficult to explain the influence of Eu(III) on the broadening of the band gap. A possible reason could be the reduced average crystallite size. It is known that the presence of Ln(III) can decrease the rate of crystal growth [36]. As shown in Table 1, the pure ZrW_2O_8 has an average crystallite size of 26 nm, while for the sample modified with 5 mol% Eu(III), it is 19 nm. The smaller crystallite size suggests quantum effects which expands the forbidden zone [37].

CONCLUSIONS

Homogeneous pure and Eu(III) modified ZrW_2O_8 samples were obtained by hydrothermal synthesis. High temperature XRD showed that the modification of ZrW_2O_8 leads to an increase of the phase transition temperature. The presence of Eu(III) causes a decrease of the coefficients of thermal expansion both for alpha- and beta-ZrW_2O_8 phases. The reversibility of the alpha-beta transition was observed by high temperature XRD. The band gap energy for pure ZrW_2O_8 was calculated from UV-Vis spectra to be 3.95 eV. The modification with Eu(III) caused an increase up to 4.45 eV.

The research presented is a part of a study in order to determine the influence of lanthanides on the properties of Zr(IV) and Hf(IV) tungstates. Future investigations will study the effect of the different lanthanide ions on the phase transition as a function of the ionic radius.

Acknowledgments: *The financial support of the Bulgarian Fund for Scientific Investigations by Contract DM 19/5 is highly acknowledged. The high temperature XRD measurements were performed at the Institute of Physical Chemistry, BAS, by Assoc. Prof. G. Avdeev.*

REFERENCES

1. M. Nazarov, D. Y. Noh, *J. Rare Earths*, **28**, 1 (2010).
2. Q. Zhang, Q. Meng, Y. Tian, X. Feng, J. Sun, S. Lu, *J. Rare Earths*, **29** (9), 815 (2011).
3. T. Liu, Q. Meng, W. Sun, *J. Rare Earths,* **33**(9), 915 (2015).
4. X. Yu, Y. Qin, M. Gao, L. Duan, Z. Jiang, L. Gou, P. Zhao, Z. Li, *J. Lumin*., **153**, 1 (2014).
5. J. Evans, T. A. Mary, T. Vogt, M. A. Subramanian, A. W. Sleight, *Chem. Mater.,* **8**(12), 2809 (1996).
6. J. Graham, A. D. Wadsley, J. H. Weymouth, L. S. Williams, *JACS*, **42** (11), 570 (1959).
7. N. Ulbrich, W. Tröger, T. Butz, P. Blaha, *Z. Naturforsch. A,* **55** (1–2), 301 (2000).
8. C. Lind, *Mater.*, **5**(6), 1125 (2012).
9. C. Georgi, H. Kern, *Ceram. Int*., 35(2), 755 (2009).
10. T. Tsuji, Y. Yamamura, N. Nakajima, *Thermochim. Acta*, **416**, 93 (2004).
11. C. Closmann, A. W. Sleight, J. C. Haygarth, *J. Solid State Chem*., **139**, 424 (1998).
12. C. De Meyer, F. Bouree, J. S. O. Evans, K. De Buysser, E. Bruneel, I. Van Driessche, S. Hoste, *J. Mater. Chem.*, **14**, 2988 (2004).
13. K. De Buysser, I. Van Driessche, B. V. Putte, P. Vanhee, J. Schaubroeck, S. Hoste, *Inorg. Chem*., **47**, 736 (2007).
14. K. De Buysser, I. Van Driessche, B. V. Putte, J. Schaubroeck, S. Hoste, *J. Solid State Chem.*, **180**(8), 2310 (2007).
15. J. Liao, S. Liu, H.-R. Wen, L. Nie, L. Zhong, *Mater. Res. Bull.*, **70**, 7 (2015).
16. Y. Yamamura, N. Nakajima, T. Tsuji, A. Kojima, Y. Kuroiwa, A. Sawada, S. Aoyagi, H. Kasatani, *Phys. Rev. B*, **70**, 104107:1 (2004).
17. A. Khan, A. A. P. Khan, A. M. Asiri, I. Khan, *J. Alloys Compd.*, **723**, 811 (2017).
18. Q. Liu, J. Yang, X. Cheng, G. Liang, X. Sun, *Ceram. Int.*, **38**, 541 (2012).
19. J. Graham, A. D. Wadsley, J. H. Weymouth, L. S. Williams, *JACS*, **42**(11), 570 (1959).
20. J. C. Chen, G. C. Huang, C. Hu, J. P. Weng, *Scr. Mater. (Scripta Metallurgica)*, **49**, 261 (2003).
21. S. Nishiyama, T. Hayashi, T. Hattori, *J. Alloys Compd*., **417**, 187 (2006).
22. J. Tani, M. Takahashi, H. Kido, *Journal European Ceramic Society*, **30**(6), 1483 (2010).
23. H. Wei, M. Hasegawa, S. Mizutani, A. Aimi, K. Fujimoto, K. Nishio, *Materials*, **11**(9), 1582 (2018).
24. N. Khazeni, B. Mavis, G. Gündüz, Ü. Çolak, *Mater. Res. Bull.*, **46**(11), 2025 (2011).
25. J. A. Colin, DeMarco V. Camper, S. D. Gates, M. D. Simon, K. L. Witker, C. Lind, *J. Solid State Chem*., **180**, 3504 (2007).

26. A. I. Gubanov, E. S. Dedova, P. E. Plyusnin, E. Y. Filatov, T. Y. Kardash, S. V. Korenev, S. N. Kulkov, *Thermochim. Acta*, **597**, 19 (2014).
27. Z. Peng, Y. Z. Sun, L. M. Peng, *Mater. Des.*, (1980–2015) **54**, 989 (2014).
28. J. Rodriguez-Carvajal, International Union for Crystallography, Newletter, N°20 (1998).
29. J. Huang, A. Sleight, Golden Book of Phase Transitions, Wroclaw, vol. 1, 2002, pp. 1–123.
30. U. Kameswari, A. W. Sleight, J. S. O. Evans, *Int. J. Inorg. Mater.*, **2**, 333 (2000).
31. J. Tauc, *Mater. Res. Bull.*, **3**, 37 (1968).
32. H.-H. Li, J.-S. Han, H. Ma, L. Huang, X.-H. Zhao, *J. Solid State Chem*., **180**, 852 (2007).
33. R. Lacomba-Perales, J. Ruiz-Fuertes, D. Errandonea, D. Martinez-Garcia, A. Segura, *EPL*, **83**, 37002 (2008).
34. D. V. S. Muthu, B. Chen, A. W. Sleigh, J. M. Wrobel, M. B. Kruger, *Solid State Commun.*, **122**(1–2), 25 (2002).
35. P. Godlewska, E. Tomaszewicz, L. Macalik, M. Ptak, P. E. Tomaszewskic, M. Berkowski, K. Lemański, P. Solarz, P. J. Dereń, J. Hanuza, *J. Alloys Compd.*, **745**, 779 (2018).
36. J. S. Church, N. W. Cant, D. L. Trimm, *Appl. Catal*., **101**, 105 (1993).
37. D. L. Ferreira, J. C. L. Sousa, R. N. Maronesi, J. Bettini, M. A. Schiavon, A. V. N. C. Teixeira, A. G. Silva, *J. Chem. Phys.*, **147**, 154102 (2017).